The 2012 World Congress on
Advances in Civil, Environmental, and Materials Research (ACEM' 12)
Seoul, Korea, August 26-30, 2012

Internal Wind Pressures for the Design of Pipe-Framed Greenhouses

*Nam-Seok Kim[1)] and Yasushi Uematsu[2)]
[1), 2)] *Department of Architecture and Building Science, Tohoku University, Sendai 980-8579, Japan*
[1)] kim-n@hjogi.pln.archi.tohoku.ac.jp

ABSTRACT

The present study investigates the internal pressure coefficients for designing pipe-framed greenhouses commonly used in Japan. Since these greenhouses have low resistance to winds, they are often damaged or collapsed by strong winds. One of the main reasons for the damage and collapse is a lack of proper wind force coefficients for designing these structures. In our previous study, we proposed a model of the external pressure coefficient, expressed as the equivalent static load, which provides the maximum load effect. The bending moment induced in the frame at the windward column base was regarded as the most important load effect for discussing the design wind loads. In practice, however, the net wind forces acting on the walls and roofs are provided by the difference between the external and internal pressures.

In the present paper, therefore, a discussion is made of the internal pressure coefficient to be combined with the proposed external pressure coefficient in the structural design. Not only an isolated model but also two or three models arranged in parallel are tested. The internal pressure coefficient is numerically simulated by using the time history of external pressure coefficients obtained from a simultaneous pressure measurement at many points along the small gaps existing in the gable and side walls. The effects of wind direction and distance between models on the internal pressure coefficient are discussed. Furthermore, the correlation between the external and internal pressures is investigated from the viewpoint of load effect. Based on these results, we propose the internal pressure coefficient for designing the structural frames of pipe-framed greenhouses.

1. INTRODUCTION

Pipe-framed greenhouses, as shown in Fig. 1, are widely used for agricultural and horticultural industries in Japan. Such greenhouses are designed to a lower level of structural safety than conventional structures, because of the need to minimize capital costs, the demand for a higher level of light transmission and so on. They are

[1)] Graduate Student
[2)] Professor

consequently very lightweight structures that are vulnerable to wind actions. In practice, they often suffer damage and collapse from typhoons and tornados (see Fig. 1(b)). One of the main reasons for such damage and collapse is a lack of proper wind force coefficients for designing these structures. Indeed, no specification of wind force coefficient is provided in codes and standards for such shapes as commonly-used greenhouses in Japan. Therefore, it is necessary to specify proper wind force coefficients. Then, Uematsu (2009) proposed a model of external pressure coefficient, expressed as the equivalent static load, based on a wind tunnel experiment. In the study, focus was on the bending moment at the windward column base of the frame as the load effect for discussing the design wind loads. The effect of internal pressure was not considered in the study.

The net wind forces acting on the walls and roofs are given by the difference between the external and internal pressures. To the authors' best knowledge, no studies have been made on the internal pressure of pipe-framed greenhouses to date. The internal pressure depends on the external pressures at the location of gaps existing in the walls as well as on the size and shape of the gaps. It is quite difficult to measure the internal pressure coefficient directly in a wind tunnel experiment because of the difficulty in model making and pressure measurements. It is also difficult to specify the size and shape of the gaps in practical structures.

In the present study, we make numerical simulations of internal pressure using the time history of external pressures measured at many points along the gaps existing in the side and gable walls of a greenhouse in a turbulent boundary layer. The external pressures are also measured at a cross-section providing the maximum load effect (bending moment of the frame at the windward column base). The location of the cross-section is determined based on our previous study (Uematsu 2009). The correlation between the load effects induced by the external and internal pressures is investigated. Based on the results, a discussion is made of the internal pressure coefficient to be combined with the model of external pressure coefficient that we proposed in our previous study. Measurements are made not only for an isolated model but also two or three models arranged in parallel. The effects of wind direction and distance between models on the internal pressure coefficient are also investigated.

(a)Typical shape (b)Collapse by typhoon

Fig. 1. Pipe-framed greenhouse commonly used in Japan

2. EXPERIMENTAL ARRANGEMENT AND PROCEDURES

The experiments were carried out in an Eiffel-type wind tunnel with a working section 4 m wide, 3 m high and 20 m long at National Institute for Rural Engineering. A turbulent boundary layer with a power law exponent of α = 0.15 for the mean velocity profile was generated on the floor by using a set of spires placed at the entrance of the working section and a number of roughness blocks distributed on the floor. The wind tunnel model is a 1:40 scale model of a typical pipe-framed greenhouse 5.4 m wide, 3.0 m high and 21.6 m long (Fig. 2). In general, the greenhouse has double sliding doors in the gable walls, as shown in Fig. 1(a). Furthermore, a part of plastic film (cladding) on the side wall can be winded up for ventilation, as shown in Fig. 3. Therefore, there exist narrow gaps around the sliding doors as well as along the lap of the films. In the wind tunnel model, many pressure taps are installed along these gaps, as shown in Fig. 2; 24 taps around each set of sliding doors 0.9 m wide and 1.8 m high in the gable wall and 18 taps along a horizontal line at a height of 0.45 m above the ground on each side wall. The time history of the external pressures at these taps is used for simulating the internal pressure. Fourteen pressure taps are also installed along a line 3.2 m inside from the gable wall (labeled 'Line A') to measure the external pressures. According to our previous study (Uematsu 2009), the external pressures along this line induce the maximum bending moment at the windward column base of a frame placed along this line, when the wind direction is 30°; the definition of wind direction θ is shown in Fig. 2. Therefore, we measure the external pressures at these 14 taps along this line. All pressure taps are connected to pressure transducers in parallel via 80 cm lengths of flexible vinyl tubing of 1 mm inside diameter. The signals from the transducers are sampled in parallel at a rate of 200 Hz on each channel for a period of 5 min. The tubing effects are numerically compensated by using the gain and phase-shift characteristics of the pressure measuring system. The mean wind velocity U_H at the height of roof top H is about 10 m/s. The velocity scale λ_V is assumed 1/3.2 for typical strong wind events, which results in a time scale of λ_T = 1/12.5. From the experimental data we obtain 5 sets of time history of pressures for a period of 10 min in full scale. The statistics of wind pressures, including the simulated internal pressure, and load effects are evaluated by applying ensemble average to the results of these five consecutive runs.

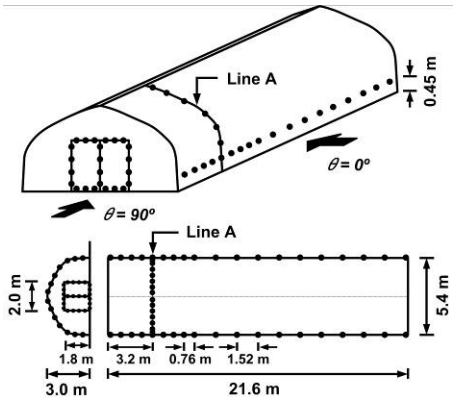

Fig. 2. Prototype of pipe-framed greenhouse

Fig. 3. Device for winding up the film

Not only an isolated model but also two or three models arranged in parallel are tested. Fig. 4 shows the arrangements of the models, in which the black model represents the instrumented model, while the white ones dummy (uninstrumented) models with the same configuration as that of the instrumented model. The gap distance *d* between models is varied from 0.25*H* to 1.0*H* (0.75 to 3.0 m). The wind direction θ is varied from 0° to 90° with an interval of 15°.

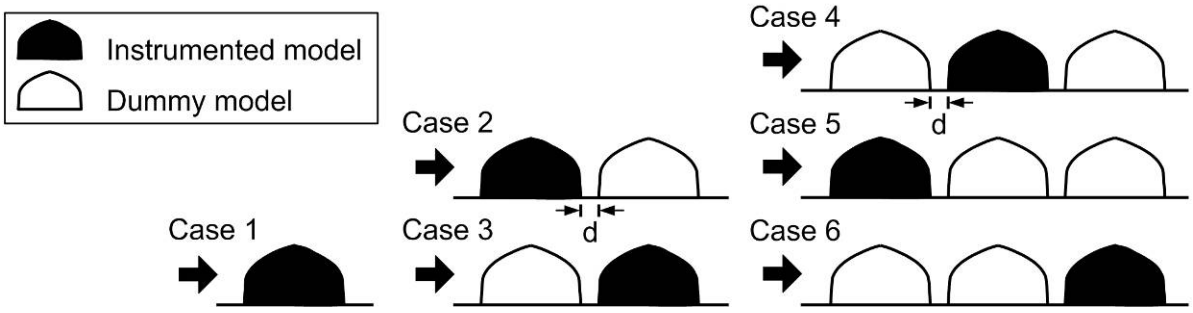

Fig. 4. Arrangements of the models tested in the experiment

3. NUMERICAL SIMULATION OF INTERNAL PRESSURE

3.1 Method of Simulation

Internal pressure is induced by the inflow and outflow through the gaps (openings) existing in the walls. Therefore, it depends on the external pressure field as well as on the location, shape, size and flow resistance of gaps (see, Holms 1979, for example). As mentioned above, there are continuous narrow gaps around the sliding doors in the gable walls and along the laps of plastic films in the side walls in a typical pipe-framed greenhouse. These continuous gaps are replaced by many discrete openings located at the pressure taps of the wind tunnel model (Fig. 2) in the simulation. The area of each opening is given by the product of the gap width and the tributary length of each pressure tap.

The present simulation is based on the unsteady Bernoulli equation, in which the opening is modeled as an orifice. The area of each opening is so small that the inertial effect of the flow can be neglected. Assuming that the gap flow is turbulent, the mass flow rate Q_j through an opening *j* may be given by the following equation (Ueda 2007) :

$$Q_j = k_j a_j U_H (C_{ej} - C_i) \mid C_{ej} - C_i \mid^{-0.5} \tag{1}$$

where k_j and a_j represent a discharge coefficient and the area of opening *j*; U_H is the mean wind speed at the level of roof top *H*; C_{ej} and C_i respectively represent the external pressure coefficient at opening *j* and the internal pressure coefficient that is assumed constant within the internal volume. The external and internal pressure coefficients C_{ej} and C_i are both defined in terms of the mean velocity pressure q_H (= $1/2\rho U_H^2$, with ρ being the air density) of the approach flow. The positive and negative Q_j represent the inflow and outflow through the gap, respectively.

For conservation of mass, the rate of mass increase inside the volume may be given by

$$\frac{d\rho}{dt} = \frac{\rho}{V_0}\sum_{j=1}^{N} Q_j \tag{2}$$

where t = time; V_0 = internal volume; and N = total number of openings in the envelop. The internal volume V_0 is assumed constant; that is, the volume change due to the deformation of the greenhouse is not considered. Assuming an adiabatic law relating the internal pressure P_i and density ρ, we obtain

$$\frac{P_i}{\rho^{\gamma}} = \text{constant} \tag{3}$$

where γ is the ratio of specific heats of air. From Eqs. (2) and (3), we obtain the following equation for the internal pressure coefficient C_i after some manipulation:

$$\frac{dC_i}{dt} = \frac{2\gamma P_0}{\rho V_0 U_H}\sum_{j=1}^{N} k_j a_j (C_{ej} - C_i)\,|\,C_{ej} - C_i\,|^{-0.5} \tag{4}$$

where P_0 is the atmospheric pressure. This equation is numerically integrated by using the Runge-Kutta method, in which the time history of external pressure coefficients C_{ej} obtained from the wind tunnel experiment is used.

3.2 Values of Parameters Used in the Simulation

The values of the parameters related to the air flows around the model and through the gaps are assumed as follows:

$$U_H = 31.5 \text{ m/s},\ \gamma = 1.4,\ \rho = 1.2 \text{ kg/m}^3,\ P_0 = 10^5 \text{ Pa}$$

The internal volume V_0 of the pipe-framed greenhouse is calculated as $V_0 = 281.9$ m^3. Few studies have been made on the gap and gap flow of pipe-framed greenhouses. Therefore, it is difficult to define the values of the parameters related to the gap flow, such as k_j. Table 1 summarizes the values of the parameters used in the present simulation, which are determined based on the previous studies together with the results of a preliminary analysis.

Table 1. Characteristics of the gap and gap flow

Location of gaps	Discharge coefficient k_j	Total gap length (cm)	Gap width (cm)	Total gap area (cm^2)	Equivalent gap area (cm^2/m^2)
Gable wall	0.65	1880	0.4	488.8	18.1
Side wall	0.50	4320	0.8	1622.4	18.1

Measurements on existing pipe-framed greenhouses indicate that the width of the gaps around sliding doors in the gable walls is approximately 4 mm. Air-tightness of the sliding doors used for pipe-framed greenhouses is lower than that for ordinary buildings. The gaps in the side walls stem from the lap of films, as shown in Fig. 5. The width of these gaps is thought to be less than 4 mm in still air. However, it is expected that the width becomes larger in strong winds because of the deformation of the films. Therefore, the width is assumed 8 mm. In this case, the equivalent gap area is 18.1 cm^2/m^2, which is about 2 times as large as that of ordinary residential houses (Murakami 1983). The effect of gap width on the internal pressure is discussed in section 4.3.

Ueda (2007) investigated the internal pressures of low-rise buildings, based on a wind tunnel experiment and a numerical simulation. They indicated that the discharge coefficient k_j was in a range from about 0.4 to 0.8 in most cases. Note that the discharge coefficient for orifice flows is typically around 0.6 (Holmes 2001). The value of k_j increases with an increase in the Reynolds number of the gap flow. We assume a lower value of k_j for the gaps in the side walls considering the gap depth. It should be mentioned that the values of k_j and the gap width used in the present simulation are tentative; further investigation of this subject is necessary.

When simulating the internal pressure coefficient by using Eq. (4), we need the initial value of C_i. The present simulation consists of two steps. In the first step, we assume that $C_i = 0$ at $t = 0$. Then, we compute the averaged value of C_i based on the simulated time history of C_i. In the second step, the mean value is used as the initial value of C_i for the simulation.

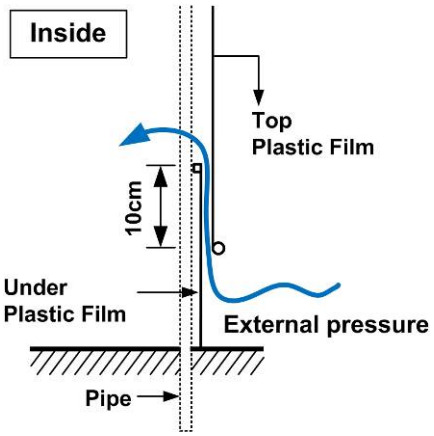

Fig. 5. Schematic illustration of gap flow through the lap of films

4. RESULTS ON INTERNAL PRESSURE COEFFICIENT FOR ISOLATED MODEL

4.1 Statistical values of Internal Pressure Coefficient

Fig. 6 shows the variation of the statistical values of internal pressure coefficient C_i with wind direction θ. The internal pressure is negative in most cases. This is due to a fact that most of the gaps exist in negative pressure areas. When $\theta = 0^o$, the minimum peak value C_{i_min} is approximately -0.33, which is the largest in magnitude. The range

of variation in C_i, from the minimum to the maximum peak value, is the largest when θ = 0°. The value of C_{i_min} increases with an increase in θ. When θ = 60°, the maximum peak value C_{i_max} is the largest, approximately 0.13. The magnitude of C_i is relatively small, less than about 0.1, when θ > 45°. The AIJ Recommendations for Loads on Buildings (2004) specifies two values of internal pressure coefficient, i.e. -0.4 and 0 for the structural frames and -0.5 and 0 for the cladding/components for ordinary buildings with no predominant openings. The estimated values of C_i in the present study is within the range of these specified values.

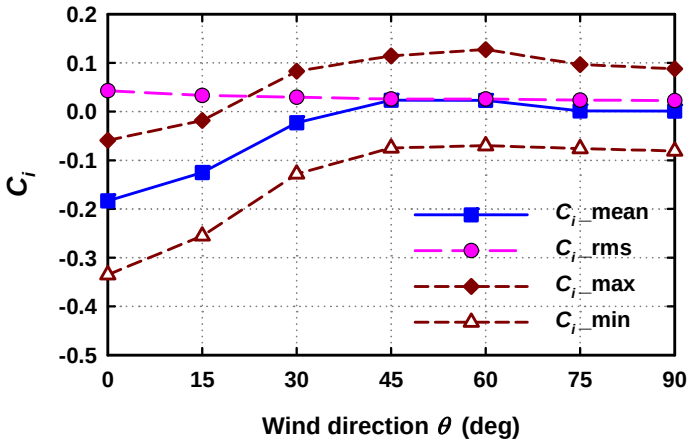

Fig. 6. Variation of internal pressure coefficient with wind direction

4.2 Correlation between External and Internal Pressures

Fig. 7 shows the relation between the internal pressure coefficient C_i and the external pressure coefficiens C_{ej} at 12 locations for θ = 30°, which is represented by the trajectory of the C_i – C_{ej} relation. Note that the wind direction of $\theta \approx$30° provides the maximum bending moment at the windward column base of a frame placed approximately 1.0H from the gable wall (see Uematsu 2009). The numerical value in each figure represents the coefficient of correlation. The value is generally low. As was mentioned in Section 3.1, the internal pressure is generated by the mass balance of the inflow and outflow. In the present model, there are many small openings in the side and gable walls. Roughly speaking, the external pressures at these points generate the internal pressure as a weighted mean. Therefore, it is thought that the correlation between the external and internal pressures at a point is low. This feature implies that a combination of the extreme values of the external and internal pressures, which is often used for practical design, is not reasonable for load estimation. Such a combination may overestimate the design wind loads.

4.3 Effect of gap size on the internal pressure coefficient

In the previous sections, we assumed that the gap size is 4 mm for the gaps around the sliding doors in the gable wall and 8 mm for the gaps along the lap of films in the side walls. In practical situations, however, the gap size may be different from these values. The change in gap size may affect the internal pressure coefficient. Hence, this effect is investigated by changing the gap size over a wide range. The tested cases are

summarizes in Table 2. Note that only the isolated model is investigated here. Fig. 8 shows the results on the statistical values of C_i plotted as a function of wind direction θ. As the size of gaps in the side walls increases, the value of C_i generally increases (decreases in magnitude). On the other hand, as the size of gaps in the gable walls increases, the value of C_i decreases (increases in magnitude). It is interesting to note that the effect of gap size on C_i is relatively small for $\theta \geq 30^o$, Considering that the external pressures induce the maximum bending moment at the windward column base when $\theta \approx 30^o$, we may conclude that the simulated results with the standard values of gap size are useful for discussing the design wind loads.

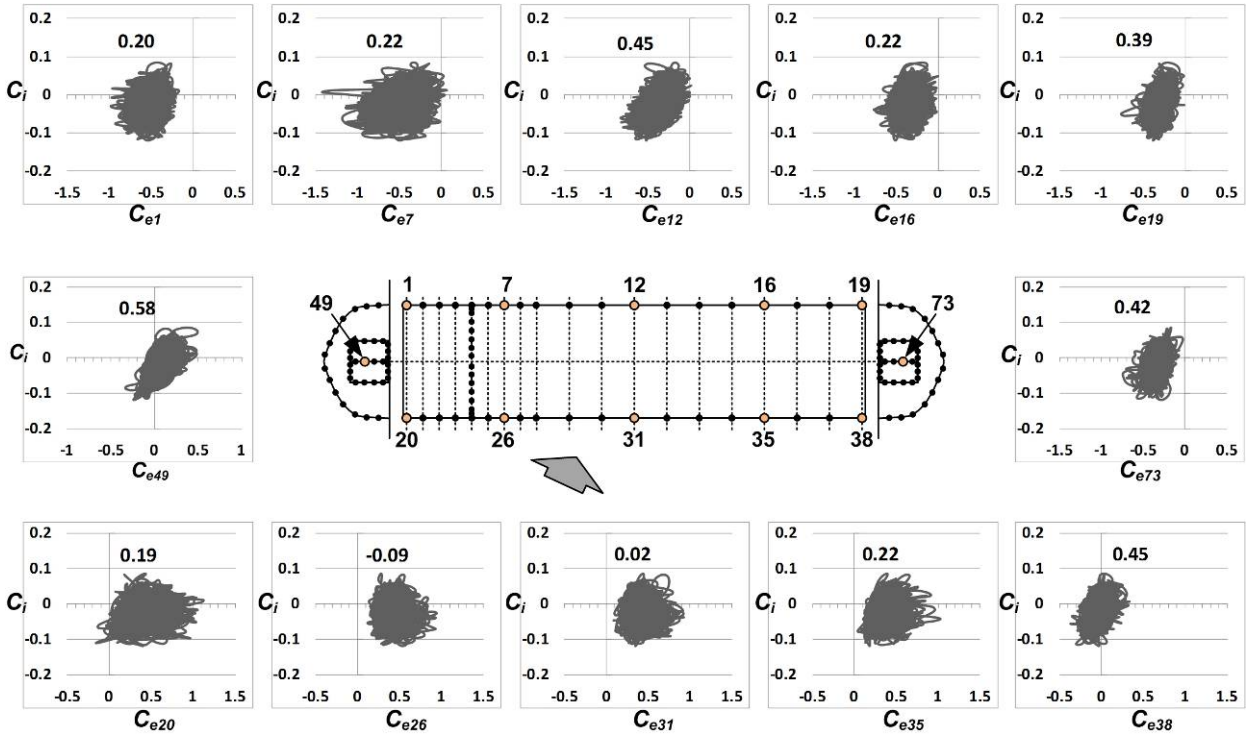

Fig. 7. Correlation between internal and external pressure ($\theta = 30^o$)

Table 2. Gap size tested

Model	Gap size (mm)	
	Side wall	Gable wall
M_{p44}	4	4
M_{p64}	6	4
M_{p84}	8	4
M_{p104}	10	4
M_{p82}	8	2
M_{p86}	8	6
M_{p88}	8	8

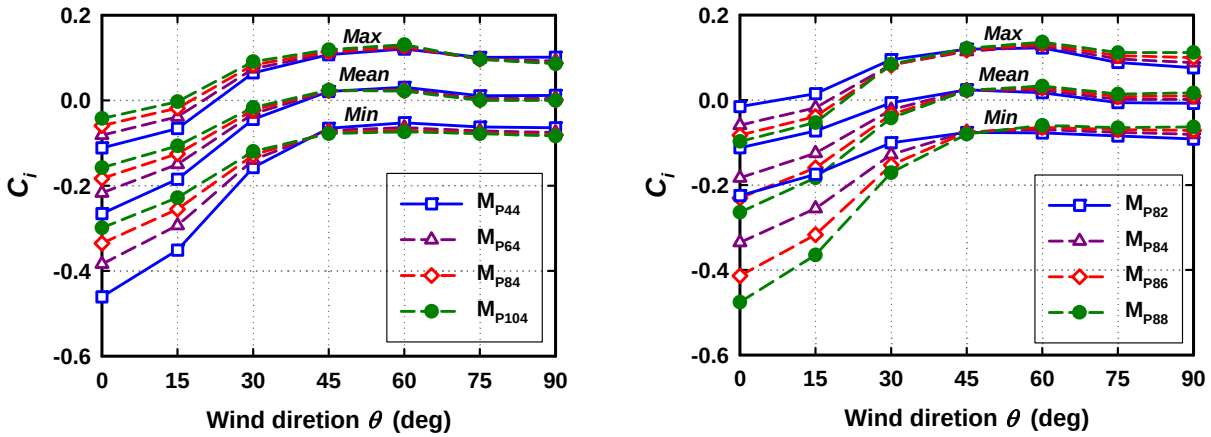

(a) Gap in the side walls (b) Gap in the gable walls

Fig. 8. Effect of gap size on the internal pressure coefficient

5. RESULTS ON LOAD EFFECTS FOR ISOLATED MODEL

5.1 General

The design wind force coefficients should be discussed based on the load effects. Considering the practical wind-induced damage to pipe-framed greenhouses (see Fig. 1(b)), the most important load effect may be the bending moment at the windward column base. Besides such a failure mode, the leeward arch pipes are sometimes pulled out from the ground, resulting in a collapse of the structure. Therefore, we focus on the bending moment M at the windward column base and the reaction N at the leeward column base of a frame located along Line A in Fig. 2, as the load effects for discussing the design wind loads.

The load effect $L(t)$, either $M(t)$ or $N(t)$, is given by the following equation, as a general expression:

$$L(t) = \sum_j q_H C_j(t) A_j \beta_j \tag{5}$$

where $C_j(t)$ represents the wind pressure coefficient (either external $C_{ej}(t)$ or internal $C_{ij}(t)$) or wind force coefficient $C_{fj}(t)$ (= $C_{ej}(t) - C_{ij}(t)$) at the location of pressure tap j; and A_j and β_j represent the tributary area and influence coefficient of pressure tap j, respectively. Note that the internal pressure coefficient $C_{ij}(t)$ is assumed constant at all tap locations, therefore $C_{ij}(t) = C_i(t)$. The bending moment $M(t)$ and the reaction $N(t)$ are normalized as follows:

$$M^*(t) = \frac{M(t)}{q_H lSH}, N^*(t) = \frac{N(t)}{q_H lS} \tag{6), (7}$$

where l represents the spacing between arch pipes; and S the width (span) of the greenhouse.

5.2 Results and Discussion

The maximum load effects induced by the external and internal pressures are plotted against wind direction θ in Fig. 9; Fig. 9(a) shows the results for the non-dimensional bending moments M_e^* and M_i^*, while Fig. 9(b) the results for the non-dimensional reactions N_e^* and N_i^*; positive reaction causes a pull-out of the arch pipe from the ground. As Uematsu (2009) pointed out, the bending moment M_e^* becomes the maximum at $\theta \approx 30^o$. On the other hand, the bending moment M_i^* induced by the internal pressure becomes the maximum at $\theta \approx 0^o$ and decreases with an increase in θ. It is found that the maximum value of M_i^* is much smaller than that of M_e^*, which implies that the internal pressure minutely contributes to the bending moment. This is due to a fact that the internal pressure fluctuates as a whole, thus inducing relatively small bending moment. The behavior of the reaction shows a similar trend with that of the bending moment. The value of N_e^* peaks at $\theta \approx 30^o$, while the value of N_i^* is the maximum at $\theta \approx 0^o$.

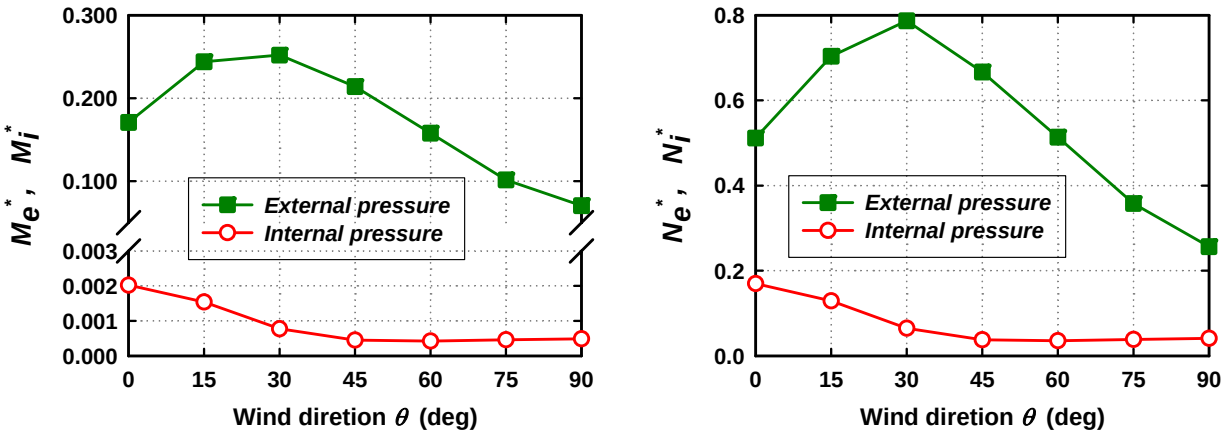

(a) Bending moment (b) Reaction

Fig. 9. Maximum load effect induced by the external and internal pressures

Fig. 10 shows the time history of M_e^* and M_i^* when θ = 30°. A phase-plane representation of M_i^* - M_e^* relation is shown in Fig. 11. The circle in the figure represents a condition that the maximum peak value of M_e^* is induced during a period of 10 min in full scale. The results for the five runs are plotted in the figure. It is found that the correlation between M_e^* and M_i^* is low; the correlation coefficient is as low as 0.31. When the M_e^* value becomes the maximum peak value, the value of M_i^* is smaller than the maximum peak value of M_i^*. This indicates that a combination of the extreme values of external and internal pressure coefficients may overestimate the design wind loads, because the maximum load effects induced by the external and internal pressures do not occur simultaneously. The correlation between the external and internal pressures should be considered from the viewpoint of load effect. Based on the result in Fig. 11, we propose that the mean $\overline{C}_i$ plus/minus twice the standard deviation σ_{Ci} of the internal pressure coefficient, represented by C_i^* (= $\overline{C}_i \pm 2\sigma_{Ci}$), is combined

with the external pressure coefficient that produces the maximum load effect. In our previous study (Uematsu 2009), we proposed a model of the external pressure coefficient C_e^* for the design of pipe-framed greenhouses, represented as the equivalent static pressure coefficient (see Fig. 12), which was based on the external pressure distribution along Line A for $\theta = 30^o$.

In order to investigate the validity of the models of external and internal pressure coefficients C_e^* and C_i^* that we proposed in the previous and present papers, the bending moment at the windward column base and reaction at the leeward column base are calculated by using the models together with a gust effect factor G_f, and compared with the actual peak values obtained from the time-history analysis for various wind directions. The results are shown in Fig. 13. The gust effect factor is defined as the ratio of the maximum peak to the mean value of the bending moment induced by the net wind forces, which is obtained from a time history analysis of the bending moment; in practice, G_f = 2.0 in the present study. The dashed line in the figure represents the predicted value from the models of C_e^* and C_i^*. It is found that the predicted value is generally larger than those obtained from the time history analysis. This result indicates that the proposed model of wind pressure coefficients can be applied to the structural design of pipe-framed greenhouses quite reasonably.

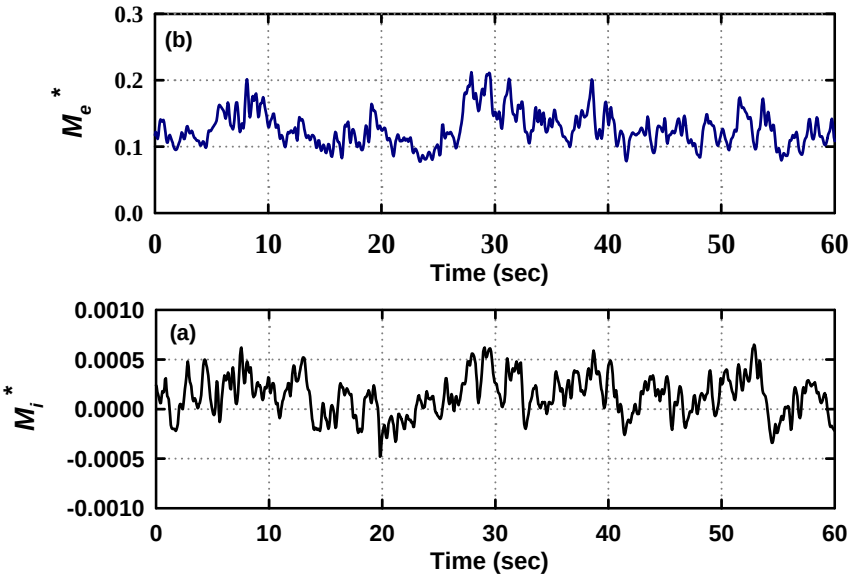

Fig. 10. Time history of non-dimensional bending moments induced external and internal pressures ($\theta = 30^o$)

6. RESULTS ON TWO OR THREE MODELS ARRANGED IN PARALLEL

6.1 Internal Pressure Coefficient

The results on the internal pressure coefficients for Cases 2 to 5 are shown in Figs. 14 to 17. In the figure, the maximum and minimum values of C_i for various values of d (gap distance between models) are plotted against wind direction θ. The result for the isolated model (Case 1) is also shown by the dashed line for the comparative purpose.

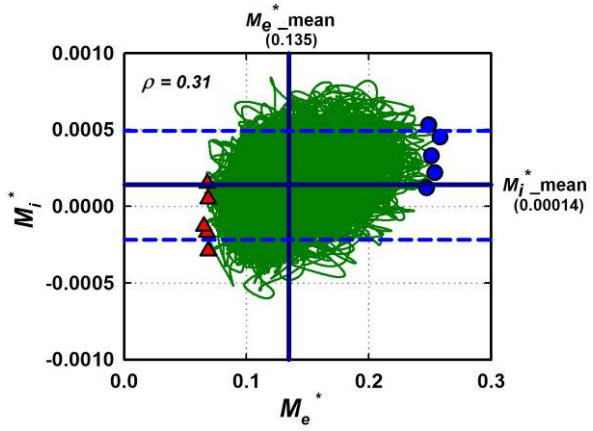

Fig. 11 Trajectory of M_e^* - M_i^* relation ($\theta = 30^o$)

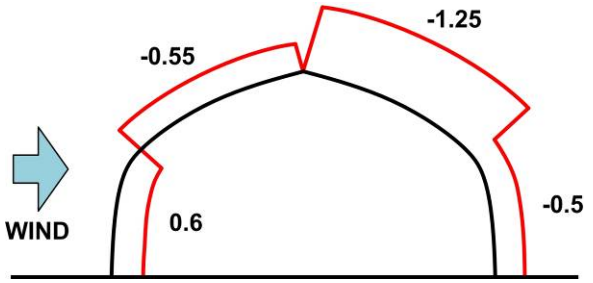

Fig. 12. Model of C_e^* (Uematsu 2009)

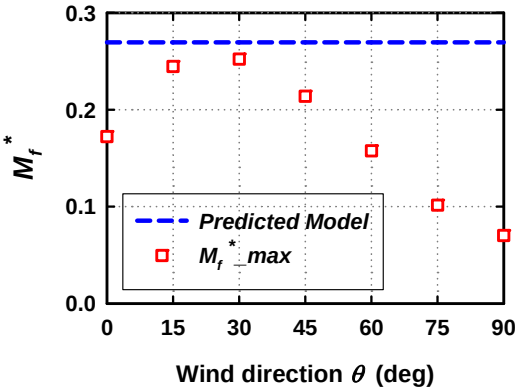

(a) Bending moment

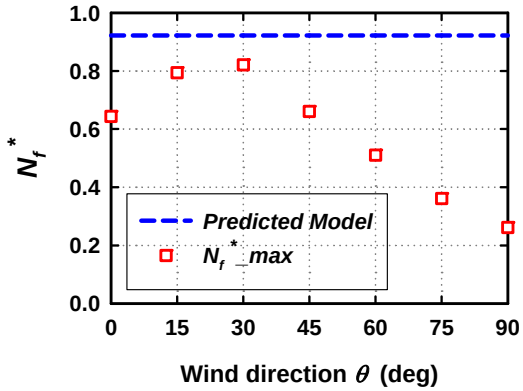

(b) Reaction

Fig. 13. Comparison between the prediction by the models of C_e^* and C_i^* and the experiment for the bending moment and reaction

The results for multiple models are rather different from that for the isolated model for $\theta \leq 60^o$, which is due to the interaction between models. On the other hand, the results for $\theta \geq 75^o$ are similar to that for the isolated model. Within the limits of the present experiment, in which the distance d between models is varied from 0.25H to 1.0H, the effect of d is not so significant. The effect of wind direction is more significant. The result for Case 5 is similar to that for Case 2, although the data for $\theta \leq 30^o$ are missing. Similarly, the result for Case 6, not shown here to save space, was found to be similar to that for Case 3.

6.2 Load effect

The maximum peak values of the non-dimensional bending moment M_f^* and reaction N_f^* are computed by using the models of C_e^* and C_i^*, and compared with the results obtained from the time history analysis. The results for Cases 2 and 3 are shown in Figs. 18 and 19. The predicted result is shown by the dashed line. In the same manner as in the isolated model case, both the bending moment and reaction for Cases 2 and 3 are smaller than the predicted value for all distances and wind directions.

The results for Cases 4 to 6 were also smaller than the predicted value. These results indicate that the models of C_e^* and C_i^* can be applied to multiple models too.

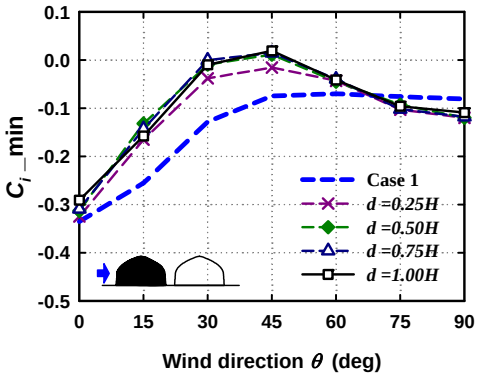

(a) Minimum peak value

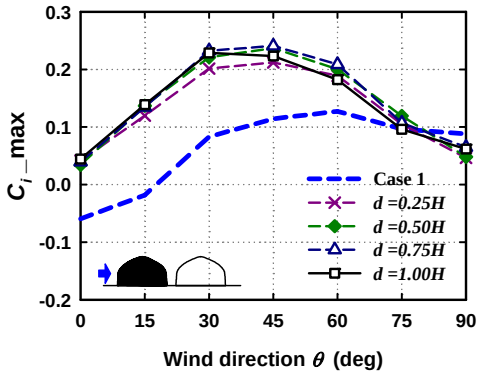

(b) Maximum peak value

Fig. 14. Variation of C_{i_min} and C_{i_max} with θ (Case 2)

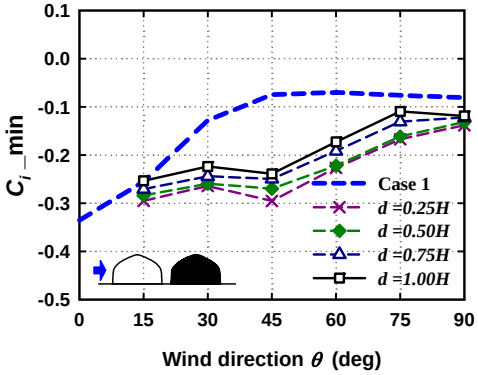

(a) Minimum peak value

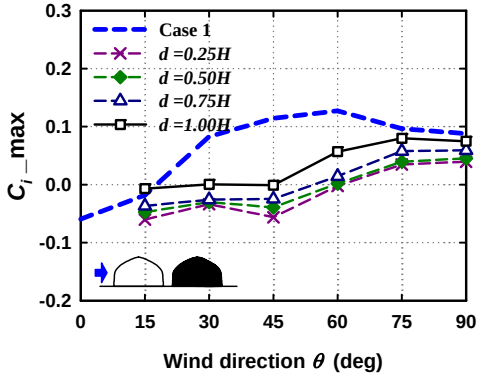

(b) Maximum peak value

Fig. 15. Variation of C_{i_min} and C_{i_max} with θ (Case 3)

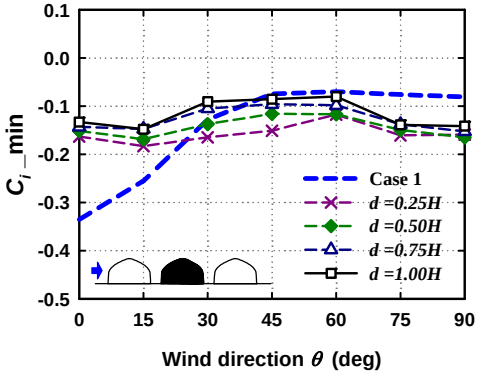

(a) Minimum peak value

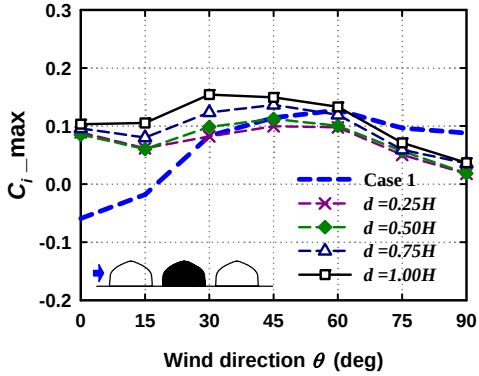

(b) Maximum peak value

Fig. 16. Variation of C_{i_min} and C_{i_max} with θ (Case 4)

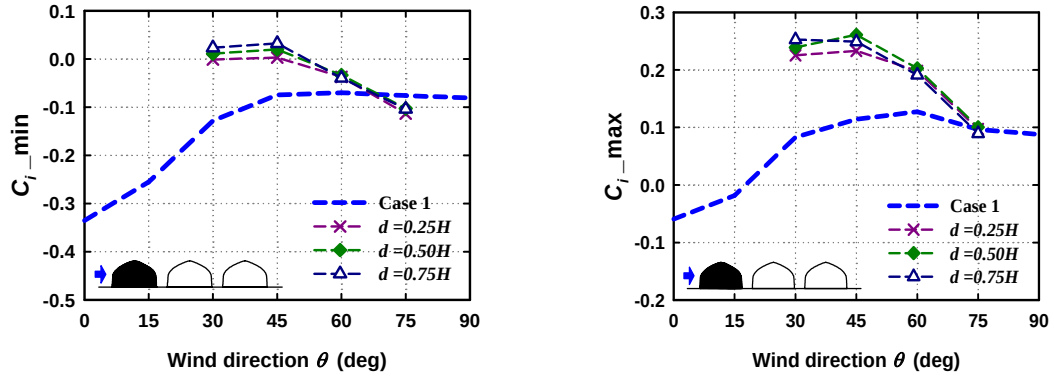

(a) Minimum peak value (b) Maximum peak value

Fig. 17. Viation of C_{i_min} and C_{i_max} with θ (Case 5)

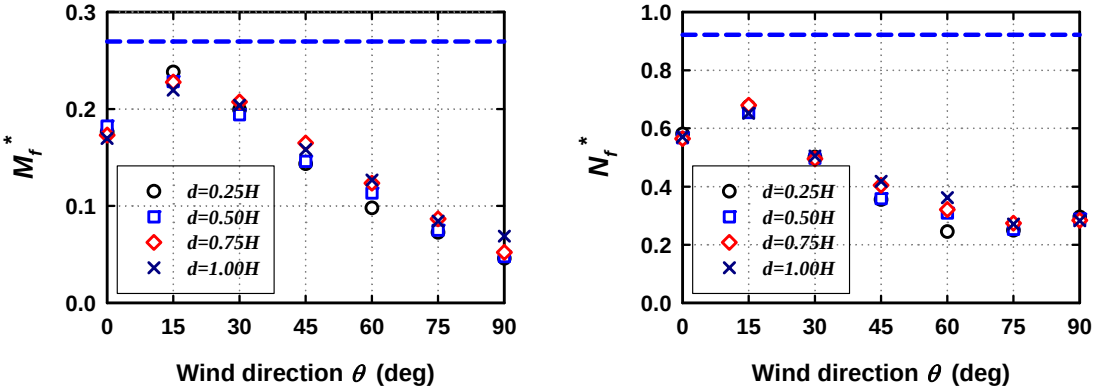

(a) Bending moment (b) Reaction

Fig. 18. Comparison between prediction and experiment for the maximum load effects (Case 2)

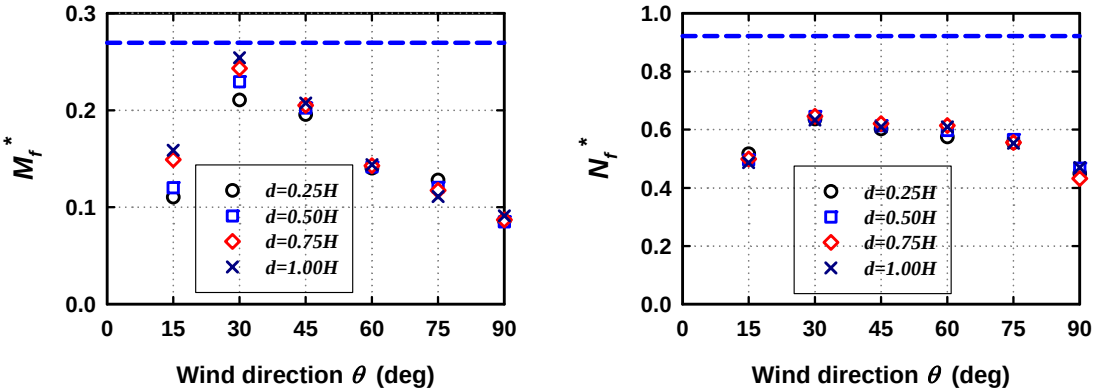

(a) Bending moment (b) Reaction

Fig. 19. Comparison between prediction and experiment for the maximum load effects (Case 3)

7. CONCLUDING REMARKS

The internal pressure induced in a pipe-framed greenhouse was investigated based on a simulation by using the time history of external pressures measured at gap locations in a turbulent boundary layer. The simulation is based on the unsteady Bernoulli equation and the conservation of mass of the air inside the volume. Not only an isolated model but also two or three models arranged in parallel were tested.

The value of internal pressure coefficient C_i varies with wind direction θ as well as with the distance d between models. The mean value of C_i ranges from about -0.2 to 0, while the peak value from -0.33 to +0.13 depending on θ and d. The minimum peak value of C_i occurs at $\theta = 0^o$, or when the wind direction is normal to the side wall. The value of C_i is relatively small when $\theta > 45^o$.

Then, the internal pressure coefficient C_i^* for designing pipe-framed greenhouses was discussed from the viewpoint of load effect. Focus was on the bending moment at the windward column base as the load effect. It is found that the correlation between the bending moments M_e and M_i induced by the external and internal pressures is fairly low. Furthermore, the magnitude of M_i is quite small compared with that of M_e. Based on the phase-plane representation of the $M_i - M_e$ relation, we proposed a model of C_i* to be combined with the model of external pressure coefficient C_e^* that we had proposed in our previous study. Indeed, C_i^* is given by the mean $\overline{C_i}$ plues/minus two times the standard deviation σ_{Ci} for $\theta = 30^o$ where the maximum load effect is induced by the wind force, i.e. pressure difference between the external and internal pressures.

Finally, the application of the proposed models of C_e and C_i was investigated by comparing the bending moment predicted by the models of C_e and C_i with that obtained from the time-history analysis for various wind directions. The predicted result is nearly equal to or larger than the results of time-history analysis not only for an isolated model but also for two or three models. This indicates that the models can be used for the structural design of pipe-framed greenhouses reasonably.

In the present paper, the values of parameters involved in the equations, such as the size and discharge coefficient of gaps, were tentatively assumed based the results of some previous investigations together with a preliminary analysis. Regarding the pipe-framed greenhouses, the data for these parameters are guite few. Therefore, future studies will be necessary to specify these parameters.

8. ACKNOWLEDGES

This study was financially supported by National Institute for Rural Engineering (NIRE). The authors are much indebted to Drs. S. Sase and H. Moriyama at NIRE for variable discussion. Acknowledgement is also due to Ms. J. Hao, who was then a graduate student of Tohoku University, for help with experiment and data processing.

REFERENCES

Architectural Institute of Japan (2004). “Recommendations for Loads on Buildings”.

Holmes, J.D. (1979). “Mean and fluctuating internal pressures Induced by wind”, Proceedings of the Fifth International Conference on Wind Engineering, Colorado State University, 435-450.

Holmes, J.D. (2001). “Wind loading of structures”, Spon Press.
Murakami S. and Yoshiro H. (1983). “Investigation of air-tightness of houses”, Transactions of the Architectural Institute of Japan, No. 325, 104-115. (in Japanese)

Murakami S. and Yoshiro H. (1983). “Investigation of air-tightness of houses”, Transactions of the Architectural Institute of Japan, No. 325, 104-115. (in Japanese)

Ueda, H., Hibi, K. and Kikuchi, H (2007). “Simulation of internal pressures in los-rise buildings induced by wind”, The Journal of Structural and Construction Engineering. Transactions of AIJ, Vol. **622**, 65-72. (in Japanese)

Uematsu, Y., Tanaka, S., Moriyama, H. and Sase, S. (2009). “External wind pressure coefficients for designing the main wind force resisting systems of pipe-framed greenhouses,” The Journal of the Society of Agricultural Structures, Japan. Vol. **40**(3), 29-38. (in Japanese)